Chapter 3

A Green perspective for the synthesis of reduced Graphene Oxide (rGO)

Contents

3.1. Introduction

Graphene which is a monoatomic thin sheet of sp^2 hybridized carbon having unique structural, optical and electrical characteristics, is utilized in a wide range of applications [1]. A. Geimand and K. Novoselov succeeded in isolating a monoatomic thin sheet of graphene using scotch tape in 2004. Since then, graphene-based research has received considerable interest [2]. The qualities of graphene are utilized in various fields like sensors, catalysis, energy conversion and storage, flexible electronics, nanoelectronics, etc. [3]. Graphene can be produced from naturally occurring graphite by mechanical or chemical exfoliation techniques [4]. The chemical exfoliation of graphite yields exfoliated graphene oxide, which is the ideal precursor for the synthesis of solution-processable graphene because of its affordability and scalability [5]. In contrast to graphene, which is insoluble in water and all organic solvents, graphene oxide (GO), which possesses high-density oxygen functionalities such hydroxyl and epoxy groups at its basal plane and carboxyl at its border, is easily soluble in water [6, 7]. In this chapter, a novel synthesis method for preparing Graphene Oxide from natural Graphite flakes and an environmentally friendly green synthesis approach for reducing graphene oxide are explained along with their characterization.

3.2. Synthesis of Highly Oxidized Graphene (HOG) by using HNO_3 and $KMnO_4$ as oxidizing agents

A two-step oxidation process was used for the synthesis of HOG. Firstly, the graphite flakes are oxidized using Nitric acid with H_2SO_4 as the intercalating agent. Secondly, it is further oxidized using $KMnO_4$ to complete the oxidation. It is then compared with GO synthesized with Hummers method and Modified Hummers method.

Materials and methodology

Graphite flake, Sulfuric acid(98%), Phosphoric Acid, Nitric Acid(70%), Potassium Permanganate, HCl, H_2O_2(30%) was bought from Merck and Sigma-Aldrich. All the reagents used were of analytical quality and were utilized as delivered.

Preparation of graphene oxide using Hummers method

2g of graphite flakes (1wt%) and 1 g of $NaNO_3$ (0.5wt%) were stirred with 70ml of H_2SO_4 in a 500ml beaker kept under ice bath (0–5ºC). The solution was constantly mixed for 2 hours at this temperature. Then 6g of $KMnO_4$ (2wt%) was introduced to the mixture gradually in 30mins time duration. After removing the ice bath, the mixture was stirred at 40 ºC for 18h until it

turned pasty brown. Then it was diluted by slowly adding 100ml DI water and the temperature was raised to 98ºC for 15min. 10ml of H_2O_2 was introduced to the mixture to eliminate the surplus $KMnO_4$ present in it. Finally, 300 ml of DI water was mixed into the mixture to dilute it and terminate the reaction. This was followed by washing of the GO sample with HCl solution and DI water repeatedly until the pH became neutral. The final filtrate was dried at 70 ºC for 24h in a vacuum oven. The resultant sample is named as GO1.

Preparation of GO using modified Hummers method

The synthesis of GO using Modified Hummers process is followed as proposed by Marcano et., al [8]. 1g of graphite flakes was mixed in a 9:1 blend of H_2SO_4 and H_3PO_4 (120:15ml) to enhance the intercalation of H_2SO_4. In addition, the amount of KMnO4 was raised from 3g to 6g for improved graphite flake oxidation. After adding $KMnO_4$, the temperature of the mixture was held at 40 ± 5 ºC for approximately 12 hours, until the solution turned brown. 50ml of DI water was added gradually while retaining a temperature of 95 ± 5ºC for about 15min. 10ml of H_2O_2 was introduced into the solution to reduce extra $KMnO_4$ present. Finally, 300 ml of DI water was mixed into the mixture to dilute it and terminate the reaction. This was followed by washing of the GO sample with HCl solution and DI water repeatedly until the pH became neutral. The final filtrate was dried at 70 ºC for 24h in a vacuum oven. The resultant sample is named as GO2.

Preparation of Highly Oxidized Graphene (HOG)

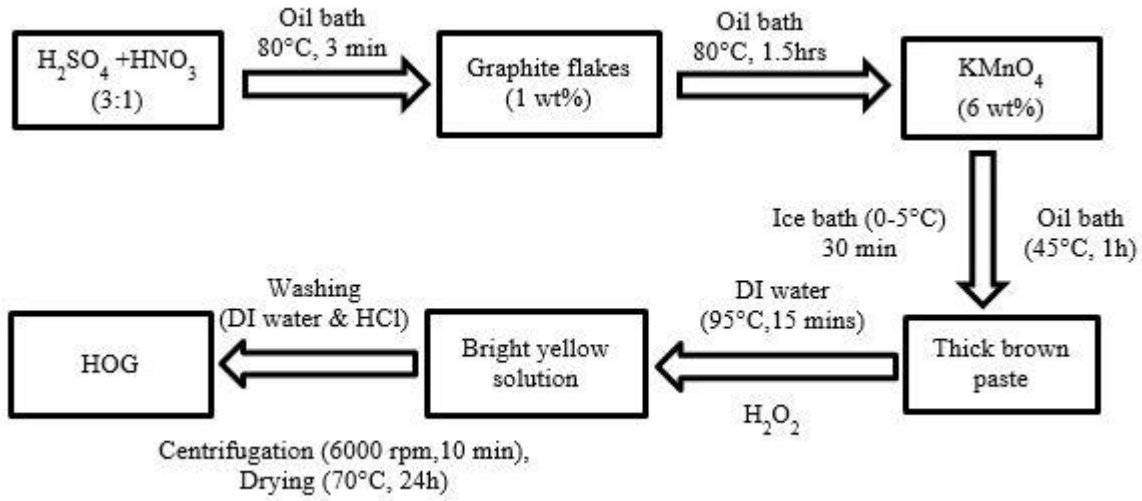

Fig.3.1. Flow chart for the synthesis of Highly Oxidized Graphene (HOG)

In this experiment GO was prepared by a 2 step chemical oxidation method. 30ml H_2SO_4 and 10ml HNO_3 (H_2SO_4: HNO_3 = 3:1) was mixed in a 500ml glass beaker placed in an oil bath at 80ºC under vigorous magnetic stirring. After 3min, 1g of graphite flakes (1wt%) was introduced into this mixture and kept stirring for 1.5h at 80ºC. This performs the initial oxidation of graphite. The vessel was subsequently placed in an ice bath (0–5 ºC) and 6g of $KMnO_4$ (6wt%) was slowly added to this solution over 30mins. Then the beaker was placed in an oil bath at 45ºC and kept under vigorous stirring for 1h, until it became a brown thick paste. Then, temperature was raised to 90ºC and 50ml of DI water was poured slowly into the solution while stirring for another 15min. Then, oil bath was removed and 4ml of H_2O_2 was introduced to the solution to reduce surplus $KMnO_4$. A bright yellow solution is obtained. This was followed by washing of the GO sample with HCl solution and DI water repeatedly until the pH became neutral. The final filtrate was dried at 70 ºC for 24h in a vacuum oven. The resultant sample is named as HOG.

Characterization

Fourier transform infrared spectroscopy (FTIR) was recorded to investigate the functional groups contained in the material using a Nicolet Impact 410 FTIR spectrophotometer. Raman spectra were recorded with RENISHAW basis series with 514 lasers. To evaluate the crystallite size and interlayer distance, X-ray diffraction (XRD) was conducted employing BRUKER AXS D8FOCUS, Cu-K_α radiation (k = 1.540598 Å), 30kV, 15mA, and a scan rate of 1º/min. UV–Vis spectroscopy was conducted employing a Thermo Scientific UV-10 Spectrometer at room temperature. Scanning electron microscopy (SEM) imaging was performed employing JEOL JSM 6390LV.

3.2.1. Results and discussions

The FTIR spectra (Fig.3.2a) of the samples shows identical functional groups for all the samples. The broad peak at 3410cm^{-1} attributes to the stretching and bending vibrations at 1380cm^{-1} of OH groups and residual water between GO sheets [9]. The absorption peak of carboxyl (C = O) was detected at 1725cm^{-1} and peak at 1620cm^{-1} attributes to stretching vibration of C = C group. The absorption peaks due to stretching vibrations of C-O at 1150cm^{-1} and C–O–C group at 1050cm^{-1} were detected in the spectra [10]. These oxygen moieties demonstrate the oxidation of graphite, and the existence of surface hydroxyl groups shows the hydrophilicity of graphene oxide.

The G-band peak is at 1605cm^{-1} and the D-band peak is at 1358cm^{-1} in the Raman spectra (Fig.3.2b) of HOG. The level of oxidation-induced defects and disorders is shown by the D-

band, while the G-band relates to the inherited graphitic domain [11]. The level of oxidation is measured by the I_D/I_G intensity ratio of the D-band and G-band peaks [12]. The I_D/I_G value of GO1, GO2 and HOG are 0.827, 0.82 and 0.86 respectively. The I_D/I_G value of HOG is the high in comparison to other samples indicating a higher degree of oxidation in comparison with others.

The XRD analysis of the synthesized GO samples was performed (Fig.3.2c) to investigate structural dissimilarities in various samples, particularly the interlayer distances. The crystalline structure and phase purity of the as-synthesized graphene oxide were evaluated using XRD analysis. In Fig.3.2c, the 9.7º diffraction peak attributes to the (001) plane of

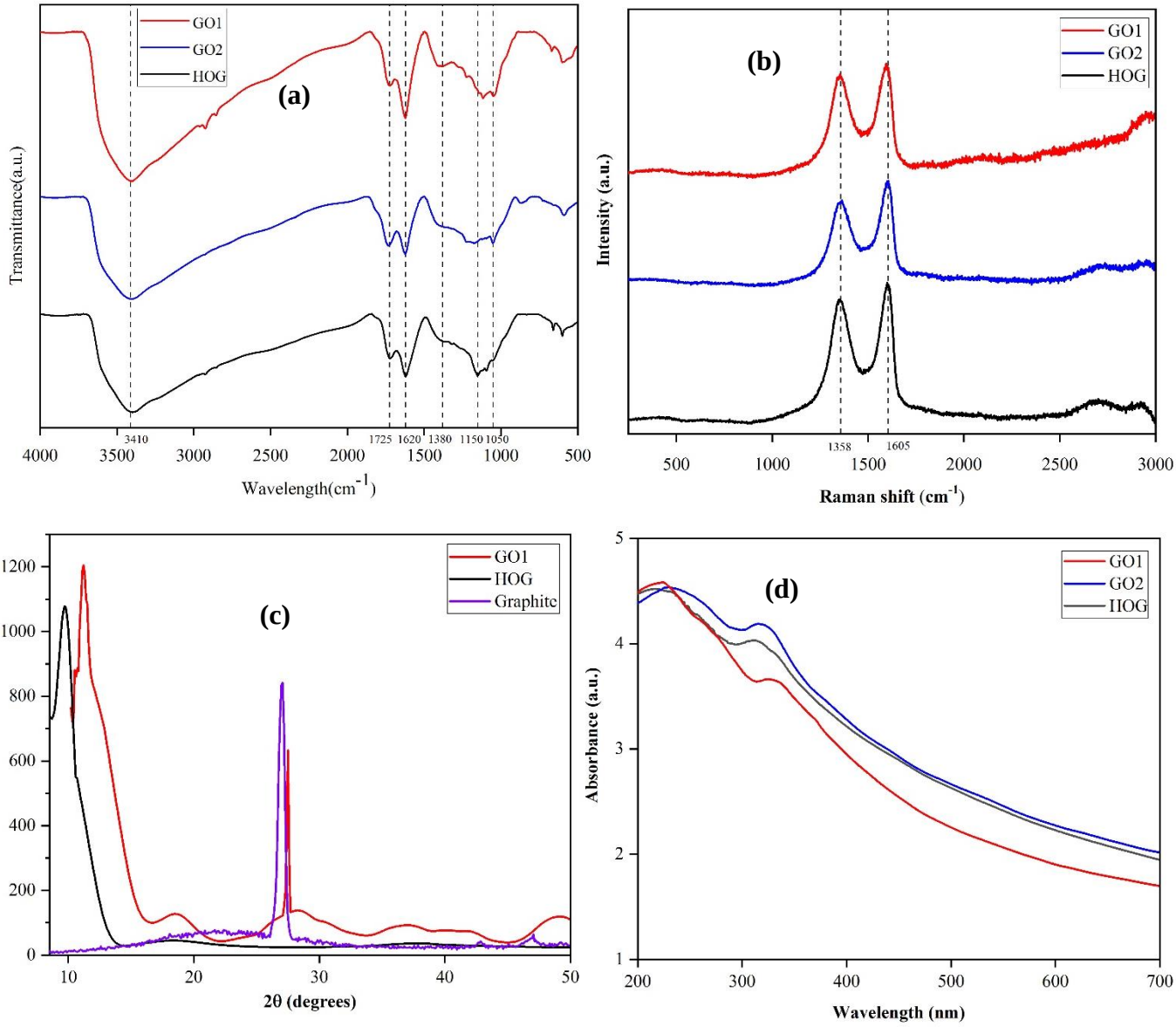

Fig. 3.2. (a) FTIR spectra of GO1, GO2 and HOG. (b) Raman spectra of GO1, GO2 and HOG. (c) XRD spectra of GO1, GO2 and HOG. (d) UV-Vis spectra of GO1, GO2 and HOG.

graphene oxide's hexagonal crystalline structure [13]. Using Bragg's law, the interlayer spacing is estimated as 9.1 Å, which is the largest ever reported for such a short synthesis time. The 2θ peak of GO1 was found to be around 11.3º; also, there is a peak around 27.6º due to the presence of unoxidized graphite particles indicating partial oxidation. In the contrary, HOG doesn't have any peak around 26º which shows complete oxidation. The increased interlayer spacing is attributable to the creation of oxygen moieties in the basal plane of GO layers and adsorbed water molecules [14]. Besides that, it is also associated with the weak Van der Waals bond formed by epoxyl, carboxyl, carbonyl and hydroxyl groups at the basal planes. The literature states that interlayer spacing, d of GO ranges from 6 to 10Å and d-spacing increases as the level of oxidation increases and quantity of water molecules intercalated into interlayer spacing [15]. According to literature, the graphite's oxidation should cause the XRD peak to shift from ~26º to ~11º [16]. The XRD analysis suggests a greater inter-planar distance, implying the HOG is highly oxidized and has a greater quantity of functional groups containing hydrophilic oxygen. The GO sheets are held together by the functional groups containing oxygen in the basal planes and the absorbed water molecules with an elevated interlayer distance [16].

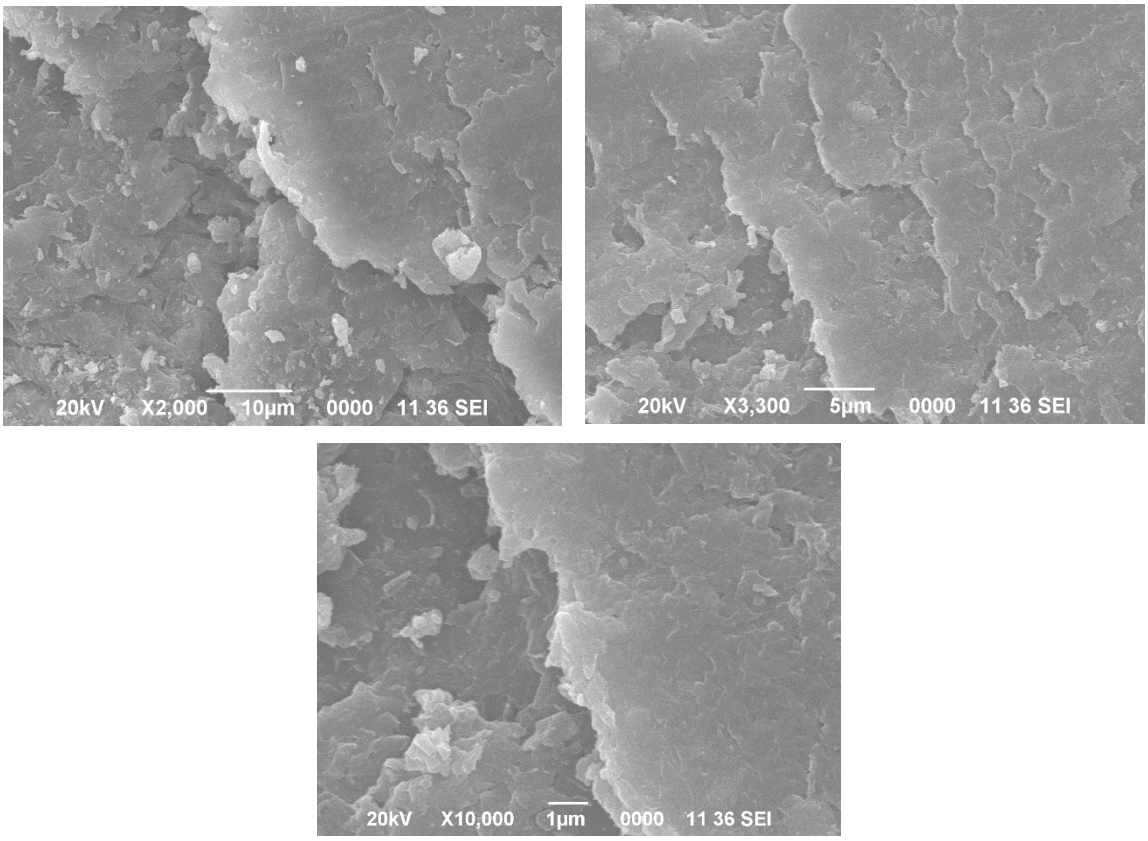

Fig. 3.3. SEM images of HOG.

The optical characteristics of the prepared GO samples were investigated using UV-Vis spectroscopy. The main peak at 220 nm (Fig.3.2d) is caused by the π-π* transitions of the C = C bond from the graphitic carbon of GO, and the shoulder peak at 310nm is because of the n-π* transitions of the C = O bond from the oxidised carbon of GO [17, 18]. Thus, the existence of oxygen moieties on graphene oxide can be seen in UV-Vis spectra, including hydroxyl, carboxyl, epoxide, and carbonyl. Thus, all samples show matching characteristics in their XRD and UV-Vis spectra, indicating that their domain structures and oxygen groups are similar. Additionally, their adsorption peaks resemble those of the GO samples described in the literature [19].

Scanning electron microscope images was employed to analyze the morphological characteristics of the synthesized HOG sample. According to SEM images (Fig. 3.3), the exfoliation and restacking processes deformed the surface, resulting in a rough surface with folds and wrinkles after oxidation [20]. These morphological changes may be the result of sp3 carbons and several GO structural defects because of the addition of functional groups containing oxygen [21, 22].

3.3. Green reduction of graphene oxide using phytochemicals extracted from Pomelo Grandis and Tamarindus indica

Graphene is said to have brought revolution to the material technology**.** There are various methods for producing high quality graphene that includes thermal exfoliation, mechanical exfoliation, chemical vapor deposition, etc. Nevertheless, the utmost efficient process for mass production is oxidizing natural graphite into graphite oxide [23, 24]. Graphene oxide (GO) is abundant in oxygen moieties; therefore, to resemble the characteristics of pure graphene, GO is further reduced to eliminate these oxygen moieties. However, the chemical reduction method utilizes strong and harmful substances like hydrazine hydrate, $NaBH_4$, hydroquinone, etc. [25, 26]. These reducing agents are extremely hazardous and dangerous in nature, which has a negative impact on the environment, and the harmful waste materials produced will increase the cost of production [27]. Therefore, more environment friendly methods must be investigated for the efficacious reduction of GO.

As a solution for this problem, green nanotechnology can be employed in which bio compatible reducing agents like Tea solution [28, 29], Holy basil [30], Wild carrot root [31], Orange peels [32], Ginseng [33], Eucalyptus leaf [34], Terminalia chebula seeds [35], Vitamin C [36], Lemon juice and Vinegar [37], Hibiscus sabdariffa L. [38], Amino acid [39], Indian gooseberry [25], Reducing sugars [40, 41], Melatonin [42], Bovine serum albumin [43][24], Bacteria [44],

Bacteriorhodopsin [45], Hydrogen-rich water [46], Curcumin [47] etc. was reported for efficient Graphene Oxide reduction. During the reduction process, Vitamin C-based reducing agents are capable of generating a highly ordered restacking structure. The surface modification of graphene with phytochemicals is an effective approach for reducing the interlayer attraction in graphene because of the Van der Waals force and preventing irreversible restacking during reduction [48, 49].

Citrus fruits are used as antioxidants from ancient times onwards. Pomelo, the largest citrus fruit with white or pinkish flesh (Citrus grandis L. Osbeck), is a member of the Rutaceae family and is a widely grown citrus fruit in the warm tropical climates. Pomelo is cultivated throughout India's southern and north eastern regions, as well as in the foothills of the Northwest of Himalayas and in parts of Orissa, Uttarakhand, Uttar Pradesh, and Bihar [50]. It contains vitamin C and a number of antioxidants, including beta-sitosterol, alkaloids, polyphenols, flavone glycosides, flavonoids, beta-carotene and terpenoids [51]. White pomelo possesses a greater antioxidative capacity than pink pomelo [52]. The phenolic compounds and ascorbic acid are responsible for the antioxidant capability of the fruit. Therefore, in this paper we have used White Pomelo juice extracts for the green reduction of GO due to its high antioxidant property.

Tamarind (*T. indica* L.) belonging to Caesalpinioideae family is widely cultivated in the Indian sub-continents. India is the largest producer of Tamarind with an annual production of 250,000 MT [53]. As per published reports, the antioxidant potential and phenolics content of Tamarind flesh is much greater than that to flesh of mango, avocado, jackfruit and longan [54]. High antioxidant potential of tamarind is well established [55], which makes it an excellent choice for green reduction of GO.

The aqueous extracts of Pomelo and Tamarind were employed for graphene oxide reduction in the current research. The prepared rGO dispersion showed good stability in water and ethanol. The reduced graphene oxide so obtained showed high conductivity. The proposed method is green and cost effective and has the potential to mass-produce graphene at a low price and without causing any environmental damage.

Materials and chemicals

Graphite flake, Sulfuric acid(98%), Phosphoric Acid, Nitric Acid(70%), Potassium Permanganate, HCl, H_2O_2 (30%) were bought from Merck and Sigma-Aldrich. All the reagents used were of analytical quality and were utilized as delivered.

Preparation of GO by oxidizing the graphite powder

GO was synthesized via modified Hummers process by oxidizing graphite flakes as previously mentioned [56]. A mixture of 30ml H_2SO_4 and 10ml HNO_3 was taken in the ratio of 3:1 and kept in an oil bath at 80ºC for 3min. Then to this solution, graphite flakes of 1g (1wt%) was added and kept under continuous stirring for 1.5h. The vessel was subsequently placed in an ice bath (0–5 ºC) and $KMnO_4$ (6g, 6wt%) was gradually introduced into it over a time span of 30min. Again the beaker was shifted to an oil bath at 45ºC for 1h (under vigorous stirring), until it turned into a thick brown paste. After that the temperature was raised to 90ºC and 50ml of DI water was poured at a slow pace, stirred for 15 more minutes and after that the oil bath was removed. For reducing the extra $KMnO_4$, 4ml of H_2O_2 was added which resulted in a bright yellow colored solution. Filtration, washing of the solution with aqueous HCl along with dialysis was carried out for neutralizing the pH. The filtrate so obtained was dried for 24h at a temperature of 70ºC in a vacuum oven. The final product is named as GO.

Preparation of Pomelo juice extract

White Pomelo was procured from the tree locally. It was cleaned with tap water for removing the soil and impurities and then air-dried. Pomelo pulp was taken out manually with the help of a sharp knife and chopped into small pieces with all the seeds being removed. The flesh was taken separately and juice was extracted using a juicer and then filtered with a sieve to remove any impurities. After that, GO is reduced using the obtained fresh extract.

Preparation of Tamarind extract

Tamarind was collected from the tree locally. The shell and the veins were removed and sticky pulp with seed was separated. Then pulp was dissolved in DI water by rubbing manually and filtered using a sieve to remove the impurities. After that, it was dried for 48h at 70ºC in a vacuum oven. The dried fruit pulp was milled into powder and was used for the reduction of GO.

Reduction of GO using aqueous phytochemicals

The prepared GO was reduced by the following procedure: 800mg of GO was mixed with 400mL (2mg/mL) of distilled water and sonicated for 1h. 200ml of GO dispersion was mixed with 100ml of Pomelo juice extract and refluxed at 95ºC for 12h. Filtering and washing of the resultant black solution was done many times with DI water to remove any impurities if present. It was then dried in a vacuum oven (70ºC, 3h) and named as P-rGO.

Similarly, 200ml of the GO dispersion was mixed with 2g of tamarind pulp powder and refluxed under the same conditions. It is named as T-rGO.

No toxic or hazardous byproducts are generated in this process as the byproducts are mainly organic compounds and water.

3.3.1. Results and discussions

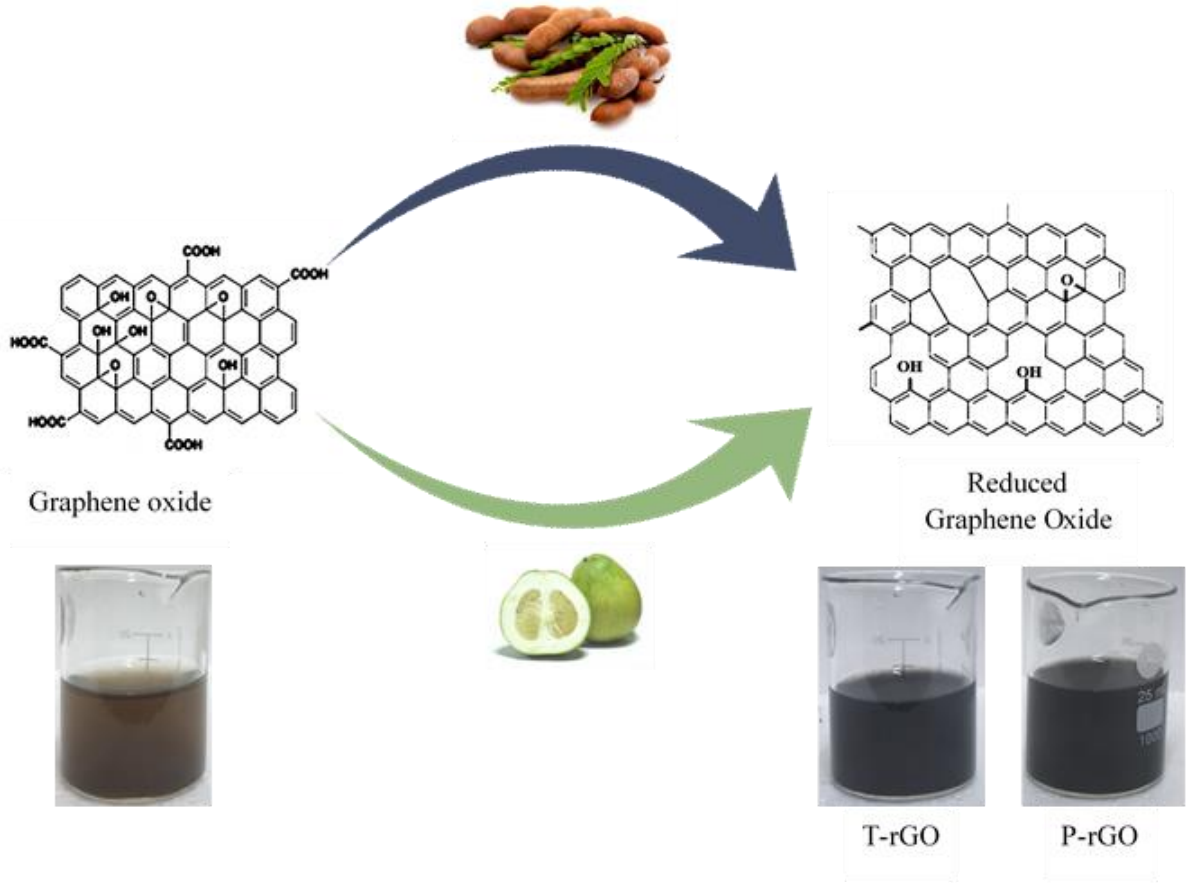

Fig.3.4. Schematic illustration for the synthesis of reduced graphene oxide

It is possible to evaluate changes in structural and electrical characteristics as a result of GO reduction by observation itself. From Fig.3.4, it is clear that the samples' color has changed from a yellowish brown to a black color, implying the complete reduction of GO. The change in color is due to the restoration of electronic conjugation and the creation of rGO. In addition, it also confirms the conversion of hydrophilic GO into hydrophobic rGO as a result of the depletion of polar functional groups on the graphene surface [57]. Further, rGO samples were found to be stable in aqueous dispersion for days. This may be due to the effect of phytochemicals acting as stabilizing or capping agents. The stability enhances the processability of rGO for subsequent applications.

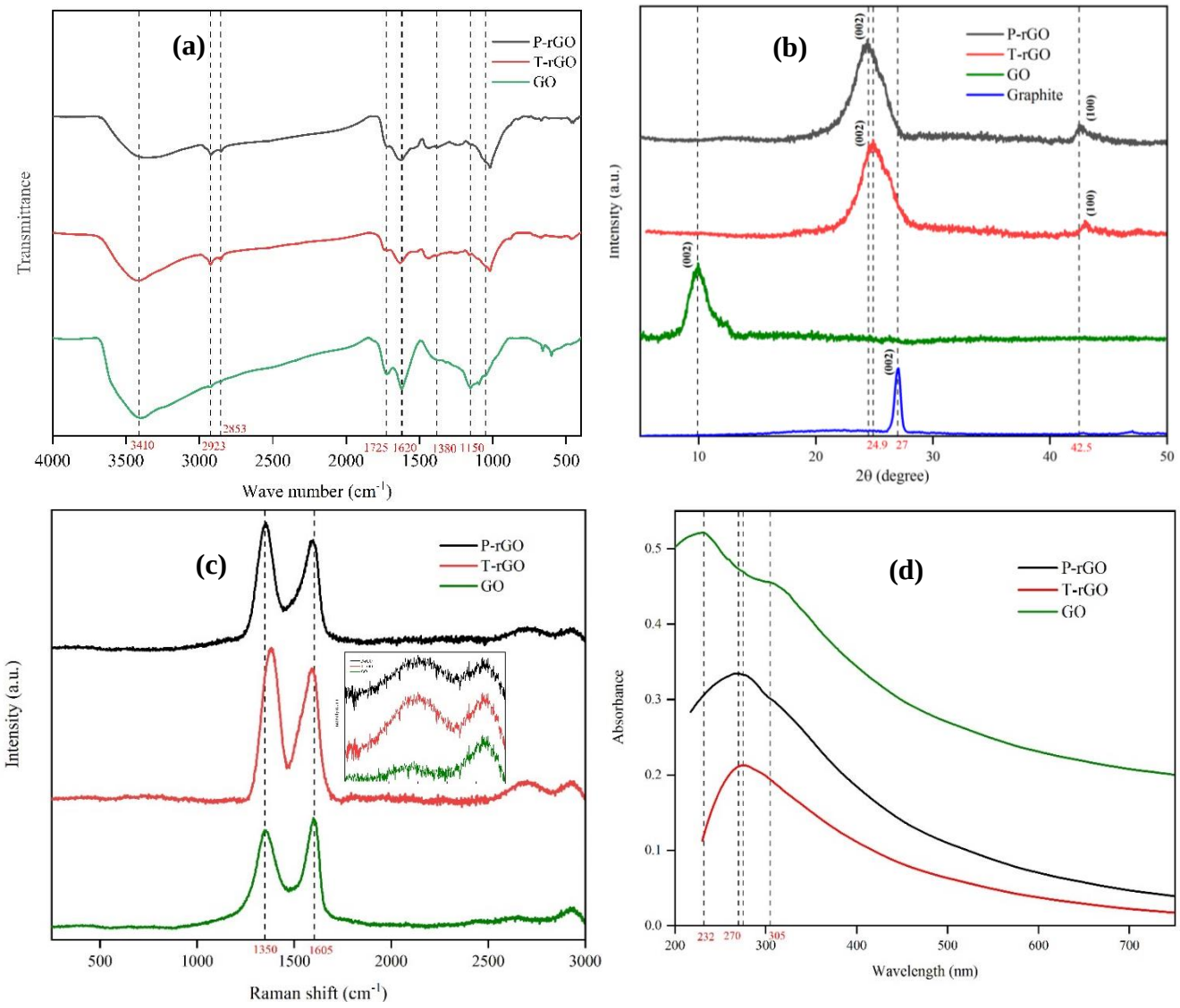

Fig. 3.5 (a) FTIR spectra of GO, P-rGO and T-rGO. (b) XRD spectra of Graphite, GO, P-rGO and T-rGO. (c) Raman spectra of GO, P-rGO and T-rGO. (d) UV-Vis spectra of GO, P-rGO and T-rGO.

To determine the degree of reduction achieved by Pomelo and Tamarind extracts, the FTIR spectra of GO, T-rGO, and P-rGO samples were analyzed. After the chemical oxidation using $KMnO_4$ and HNO_3, the basal plane of GO has functional groups which includes hydroxyl (–OH), epoxy (–O–), carbonyl (=O) and carboxyl (–COOH) in the periphery [56]. From the FTIR spectra (Fig.3.5a), a broad peak centered at 3410cm^{-1} and at 1380cm^{-1} attributing to stretching and bending of hydroxyl (–OH) group and residual water between GO sheets due to the absorbed moisture [58]. The presence of other oxygen functionalities were found with absorption peaks centered at 1725cm^{-1}, 1620cm^{-1}, 1150cm^{-1} and 1050cm^{-1} attributes to C=O

stretching, C=C (skeletal vibration from sp^2 carbon rings), C-O-C and C–O groups respectively [59]. The characteristic peaks at 2923cm^{-1} and 2853cm^{-1} are attributed to the adsorption of phytochemicals containing phenolic groups onto the surface of graphene sheets for both rGO samples [60]. This gives proof for the phytochemicals acting as stabilizing or capping agents, which gives stability for rGO in aqueous suspension [61]. After the reduction process, peak at 1150cm^{-1} for (C-O-C) totally disappeared. However, the intensity of the carbonyl group (C=C) in rGO samples did not reduce significantly. This indicates the restoration of C=C skeletal vibration following a successful reduction procedure [62]. In addition, the strength of functional groups containing oxygen was significantly diminished in comparison to GO, confirming the effectiveness of fruit extracts in reducing GO.

Powder XRD gives information about crystallinity, average crystal size and interlayer distance of the material. From the XRD spectra, the d-spacing is determined for all samples using the Bragg's law:

$$n\lambda = 2d \sin\theta$$

where, n represents the "order" of reflection, λ is the wavelength of the incident X-rays, θ is the angle of incidence and d is the interlayer distance. The (002) basal plane reflection peak at 27˚ of raw graphite attributes to a d-spacing of 3.39 Å [63]. From Fig.3.5b, after chemical oxidation of pristine graphite, the characterized peak disappears from 27˚ and re-appears at a smaller angle of 9.9˚, corresponding to an interlayer distance of 8.96 Å. The peak at 9.9˚ is the reflection of (002) plane of the hexagonal crystalline phase of GO. The fact that there is only one XRD peak indicates that the graphite has completely oxidized. The increase in interlayer distance of GO than that of pristine graphite is mainly attributes to the incorporation of functional groups containing oxygen onto the surface of graphene layers [64]. Nevertheless, following the reduction process, the peak of T-rGO at 2θ=24.9˚ (d spacing=3.66 Å) and P-rGO at 2θ= 24.5˚ (d spacing= 3.71Å) was detected, while peak of GO at 2θ= 9.9˚ vanished. The reduction in d-spacing is because of the efficient exclusion of functional group containing oxygen following the reduction process. The elimination of functional group having oxygen is consistent with the FTIR findings that were covered in the section above. In addition, peaks are observed at around 42.5˚ which corresponds to the reflection from (100) plane. The interlayer distance of rGO synthesized is close to that of graphite (3.39 A˚) as previously reported in literature [65]. This indicates the successful creation of rGO nanosheets with a few layers of thickness after treating GO with the phytochemicals.

Raman spectroscopy is extremely useful for characterizing graphitic nanomaterials (Fig.3.5c). It gives details regarding the degree of chemical modification, crystallinity, and crystal

disorder, among other characteristics [64]. In Raman spectra, the G band signifies the first-order scattering of the E_{2g} mode by sp^2 carbon at the Brillouin zone centre, which is the inherited graphitic domain and D-band characterizes the level of defects and disorder induced by the incorporation of functional groups onto the graphene surface during the oxidation process. The degree of oxidation is evaluated by the I_D/I_G intensity ratio of D-band to G-band peaks [11, 65]. The Raman spectral data of GO reveals a D-band peak at 1350cm^{-1} and a G-band peak at 1605cm^{-1}. While G-band and D-band peak for T-rGO are at 1383cm^{-1} and 1590cm^{-1} and that for P-rGO are at 1355cm^{-1} and 1598cm^{-1} respectively. The G band and D band are broadened and moved closer for both the rGO samples. This corresponds to the restoration of electronic conjugation between graphene layers and restacking, as expulsion of oxygen functionalities permits the rGO to associate and restack after successful reduction [12]. The I_D/I_G values of GO, T-rGO and P-rGO are 0.86, 1.16 and 1.137 respectively. The intensity ratio increased significantly for T-rGO and P-rGO than that of GO. This implies the rise in the level of disorder after the reduction process and the existence of more small-sized, isolated in-plane sp^2 graphene domains in rGO [66]. Single-layer graphene can be differentiated from multi-layer graphene based on the shape and location of the 2D band [44]. The Lorentzian peak for the 2D band in graphene with single layer is located at 2679cm^{-1}. This peak will broaden and shifts (19cm^{-1}) to higher wave number for multilayer graphene (2-4 layers) [45]. The GO contains many functional groups that prevent the graphene layer from stacking but after the elimination of such functional groups, the graphene layers may restack and forms few layer rGO [32]. The 2D peak for GO was found to be at 2692cm^{-1} which that single layer sheets were present in GO suspension [42]. The 2D peaks of rGO was found to be at around 2700cm^{-1}, which (~19cm^{-1} shift) implies the formation of multilayered (2-4 layers) graphene nanosheets. The 2D mode defines the aromatic carbon structure and (D+G) mode gives information about the lattice induced disorder in the graphitic structure [64]. The rGO peaks for 2D and (D+G) modes were seen at 2700cm^{-1} and 2936cm^{-1} respectively. The $I_{2D}/I_{(D+G)}$ ratio of rGO is significantly greater in comparison to GO, implying the successful restoration of aromatic carbon structure upon reduction of GO using phytoextracts [67].

UV- Vis spectroscopic analysis of all the samples were obtained in the spectral range of 200-800nm. From fig.3.5d, two main absorption peaks can be observed for GO. The predominant peak at 232nm is caused by the π-π^* transitions of the C = C bond from the graphitic carbon of GO, and the shoulder peak at 305nm is caused by the n-π^* transitions of the C = O bond from

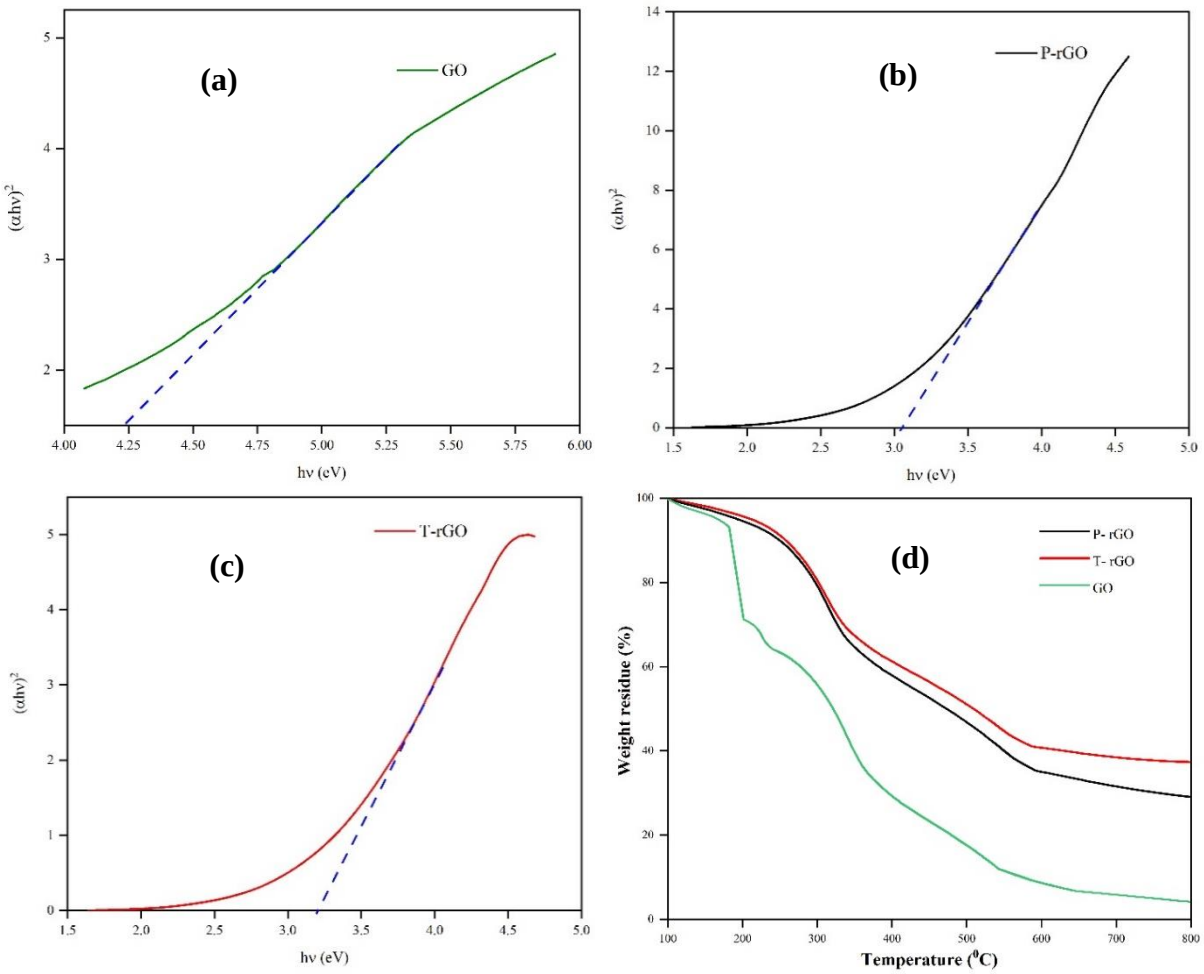

Fig. 3.6. Tauc plot of (a) GO (b) P-rGO (c) T-rGO (d) TGA of GO, P-rGO, T-rGO

the oxidised carbon of GO [17, 68]. Following the reduction process, the characteristic peak of GO at 232nm were red-shifted to 270nm for P-rGO and 275nm for T-rGO. In addition, the absorption peak at 305nm disappeared for both the rGO samples. The red shift in the wavelength suggests the structural restoration of sp^2-hybridized carbon atoms and the elimination of oxygen-containing moieties because of which electrons requires lesser energy for excitation [18, 69]. All these results points towards the efficient reduction of GO.

Using UV-visible spectra, the following formula was employed to determine the band gap energy of GO and rGO [70]:

$$\alpha = \frac{C(h\vartheta - E_{bulk})^{1/2}}{h\vartheta}$$

where, α is absorption coefficient, C is a constant, $h\vartheta$ is the photon energy and E_{bulk} is bulk 'band gap'. In the plot of $h\vartheta$ versus $(\alpha h\vartheta)^2$ in Fig.3.6(a-c), the band gaps were calculated by extrapolating a linear regression to $(\alpha h\vartheta)^2$=0. The obtained band gaps of GO, P-rGO, and T-

rGO are 4.2, 3.1, and 3.2 eV, respectively, which are consistent with previously published reports [71].

Thermogravimetric method was employed to analyze the thermal stability of GO, P-rGO and T-rGO (Fig.3.6d). The minute weight reduction at about 100˚C is due to the vaporization of residual water molecules remained in the samples after drying. GO exhibits weight loss at two stages. The initial weight loss at around 175˚C is caused by the elimination of hydroxyl, epoxy functionalities and residual water molecules. The second stage of weight loss occurs between 450 and 550˚C because of the thermal decomposition of remaining oxygen moieties and ring carbons to produce CO and CO_2 [72]. In the contrast, rGO showed much better thermal stability than GO. rGO exhibited around 10-12% weight loss at 250˚C while GO exhibited about 40% weight loss. This suggests a significantly smaller amount of oxygen moieties than GO. The lesser mass-loss is attributed to the higher degree of reduction.

SEM imaging was done to further examine the surface morphologies of the samples. From fig.3.7a, the SEM images reveals that the GO surface have a corrugated morphology with wrinkles and folds [73]. These deformities on the graphene surface corresponds to the incorporation of oxygen functionalities after the chemical oxidation process and the exfoliation and restacking processes occurred thereby [74]. From Fig.3.7b and Fig.3.7c, wrinkles and folds were altered in contrast to the surface morphology of GO after reduction process and randomly aggregated, small sized sheets were formed which are closely associated with each other. This change in morphology is because of the expulsion of labile oxygen moieties and the restoration and restacking of graphene sheets [22]. This morphological distinction indicates that rGO contains more defects and isolated graphene domains than GO [65], which has already been proved with the Raman and XRD results. It can be observed that P-rGO has more stacked layers than T-rGO, whereas T-rGO has more small-sized sheets with curled edges than P-rGO. The eradication of covalent bonded oxygen moieties from the basal planes and edges during the reduction procedure, results in the restoration of graphene sheets where the sheets are held together by the Van der Waals force of attraction. During this restoration and restacking process, the graphene sheets are crumpled with each other and as a result small-sized graphene plates are formed. The SEM results are in conjunction with Raman and XRD results.

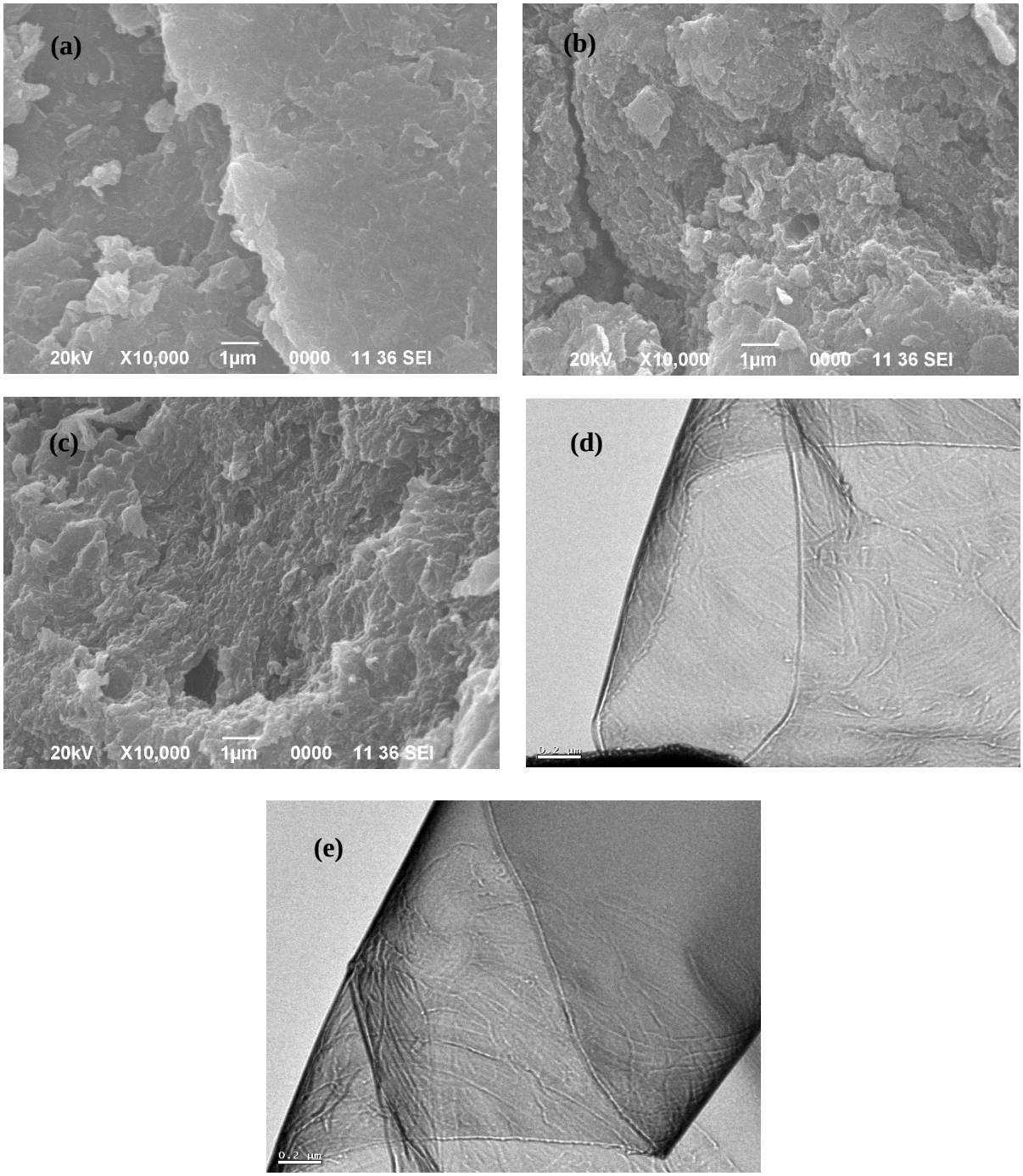

Fig. 3.7. SEM images of (a) GO (b) P-rGO (c) T-rGO and TEM images of (d) T-rGO (e) P-rGO

Fig.3.7(d,e) illustrates the TEM morphology of T-rGO and P-rGO. The rGO exhibits a sheet like morphology with high transparency due to the atomic size thickness of the samples [47]. The rGO sheets are transparent with clearly visible wrinkles and curled edges, indicating that the achieved rGO consists primarily of a single or a few layers of graphene [75]. The wrinkles developed as a result of the relaxation of strain on the C-C bond in the epoxy groups during the

development of three-membered epoxide rings in GO, and the folding is related to the existence of isolated hydroxyl and epoxy groups [25]. These morphological appearance confirms the reduction of GO in both samples.

The elemental composition of GO, P-rGO and T-rGO were studied by elemental analysis. Carbon to Oxygen ratio (C/O) of T-rGO, P-rGO and GO were found to be 7.33, 6.82 and 2.21 respectively [32]. The higher C/O value of rGO in comparison with GO implies that lesser amount of Oxygen content is present in rGO sample after reduction. These findings support the TGA conclusions and further confirms the efficient reduction of GO using fruit extracts.

The degree of reduction and restoration of the π-conjugated structure can be established by evaluating the electrical conductivity of rGO. The four probe arrangement was employed to measure the sheet resistance. The average conductivities of P-rGO, T-rGO, and GO were determined to be 4090 ±164 Sm^{-1}, 5545 ±173 Sm^{-1} and 6 Sm^{-1}, respectively. The conductivity of rGO increased 10^4 times than GO after reduction and the acquired results concurred with previously reported findings [36].

The phytoextracts have the ability of reducing oxygen functionalities present in GO. This is due to the conversion of phytochemicals to its corresponding quinones [32]. As mentioned earlier, both Pomelo and Tamarind are rich in reducing agents like ascorbic acid, polyphenols, etc., which can be easily oxidised. The chemical reduction of GO can be theorized as a 2 step SN2 nucleophilic process proceeded by a thermal elimination procedure. The GO mainly consists of 3 types of reactive functional groups on its periphery namely epoxide, hydroxyl and carbonyl. The electron pulling back effect of 5 or 6 membered rings of L-ascorbic acid/polyphenol present in the phytoextracts makes the hydroxyl group more acidic. This makes L-ascorbic acid/polyphenols to readily disassociate two protons and thus act as a nucleophile [36]. The epoxide undergoes a ring opening reaction when the L-ascorbic acid's oxygen anion takes part in a SN2 nucleophilic attack. Backside SN2 nucleophilic attack may follow the reduction process, which yields water molecule and results in intermediate compound formation. Lastly, the intermediate compound may experience thermal elimination, resulting in the creation of rGO [32]. The carbonyl and hydroxyl groups likewise undergo a similar nucleophilic attack by the polyphenols' oxygen anion and are subsequently further reduced by thermal elimination.

3.4. Conclusion

The proposed process for GO synthesis has significant advantages over the Hummers method or modified Hummers method. The XRD and Raman spectroscopic results reveals that the proposed method produced a higher amount of well oxidized GO than other methods. The synthesis time has been drastically reduced compared to other methods. The dispersibility, chemical structures, physical properties, and morphology of GO synthesized by both the proposed and Hummers procedures are nearly identical. The yield of the overall reaction is not affected by the exclusion of $NaNO_3$. Overall, these findings imply that the suggested approach is suitable for large-scale GO synthesis. In addition, it may serve as a harbinger for the development of diverse workup methods for obtaining single-layer graphene and its derivatives for supercapacitor applications, hydrogen storage, biosensors, nanofiltration membranes, ion conductors, etc.

In addition, a simple and ecofriendly synthesis technique for reducing graphene oxide using phytochemical extracts of Pomelo Grandis and Tamarind has been reported. The process does not produce any toxic or hazardous byproducts, as the byproducts are mainly organic compounds and water. The main benefits of the phytochemicals are their non-toxicity, wide availability, easy extraction process and low cost. The approach is shown to be highly effective at removing oxygen moieties from GO and is scalable. The results shows the formation of well-organized, layered rGO. The graphene electrodes exhibited high carbon to oxygen ratio (7.33, 6.82) and good electrical conductivity (5545-4090 Sm^{-1}). The prepared rGO dispersion showed good stability in water and ethanol. The proposed technique is green and cost effective and has the potential to mass-produce graphene at a low price and without causing any environmental damage.

Bibliography

[1] Li, X., Zhu, Y., Cai, W., Borysiak, M., Han, B., Chen, D., Piner, R. D., Colombo, L. and Ruoff, R. S. Transfer of large-area graphene films for high-performance transparent conductive electrodes. *Nano letters,* 9(12):4359-4363, 2009.

[2] Novoselov, K. S., Geim, A. K., Morozov, S. V., Jiang, D.-e., Zhang, Y., Dubonos, S. V., Grigorieva, I. V. and Firsov, A. A. Electric field effect in atomically thin carbon films. *science,* 306(5696):666-669, 2004.

[3] Chen, J., Yao, B., Li, C. and Shi, G. An improved Hummers method for eco-friendly synthesis of graphene oxide. *Carbon,* 64:225-229, 2013.

[4] Segal, M. Selling graphene by the ton. *Nature nanotechnology,* 4(10):612-614, 2009.

[5] Konios, D., Stylianakis, M. M., Stratakis, E. and Kymakis, E. Dispersion behaviour of graphene oxide and reduced graphene oxide. *Journal of colloid and interface science,* 430:108-112, 2014.

[6] Eigler, S. and Hirsch, A. Chemistry with graphene and graphene oxide—challenges for synthetic chemists. *Angewandte Chemie International Edition,* 53(30):7720-7738, 2014.

[7] Dreyer, D. R., Park, S., Bielawski, C. W. and Ruoff, R. S. The chemistry of graphene oxide. *Chemical society reviews,* 39(1):228-240, 2010.

[8] Marcano, D. C., Kosynkin, D. V., Berlin, J. M., Sinitskii, A., Sun, Z., Slesarev, A., Alemany, L. B., Lu, W. and Tour, J. M. Improved synthesis of graphene oxide. *ACS nano,* 4(8):4806-4814, 2010.

[9] Alam, S. N., Sharma, N. and Kumar, L. Synthesis of graphene oxide (GO) by modified hummers method and its thermal reduction to obtain reduced graphene oxide (rGO). *Graphene,* 6(1):1-18, 2017.

[10] Krishnamoorthy, K., Veerapandian, M., Yun, K. and Kim, S.-J. The chemical and structural analysis of graphene oxide with different degrees of oxidation. *Carbon,* 53:38-49, 2013.

[11] Hu, Y., Song, S. and Lopez-Valdivieso, A. Effects of oxidation on the defect of reduced graphene oxides in graphene preparation. *Journal of colloid and interface science,* 450:68-73, 2015.

[12] Liu, Z., Duan, X., Zhou, X., Qian, G., Zhou, J. and Yuan, W. Controlling and formation mechanism of oxygen-containing groups on graphite oxide. *Industrial & Engineering Chemistry Research,* 53(1):253-258, 2014.

[13] Chen, J., Li, Y., Huang, L., Li, C. and Shi, G. High-yield preparation of graphene oxide from small graphite flakes via an improved Hummers method with a simple purification process. *Carbon,* 81:826-834, 2015.

[14] Loryuenyong, V., Totepvimarn, K., Eimburanapravat, P., Boonchompoo, W. and Buasri, A. Preparation and characterization of reduced graphene oxide sheets via water-based exfoliation and reduction methods. *Advances in Materials Science and Engineering,* 2013, 2013.

[15] Ramesh, P., Bhagyalakshmi, S. and Sampath, S. Preparation and physicochemical and electrochemical characterization of exfoliated graphite oxide. *Journal of colloid and interface science,* 274(1):95-102, 2004.

[16] Al-Gaashani, R., Najjar, A., Zakaria, Y., Mansour, S. and Atieh, M. XPS and structural studies of high quality graphene oxide and reduced graphene oxide prepared by different chemical oxidation methods. *Ceramics International,* 45(11):14439-14448, 2019.

[17] Li, D., Müller, M. B., Gilje, S., Kaner, R. B. and Wallace, G. G. Processable aqueous dispersions of graphene nanosheets. *Nature nanotechnology,* 3(2):101-105, 2008.

[18] Lai, Q., Zhu, S., Luo, X., Zou, M. and Huang, S. Ultraviolet-visible spectroscopy of graphene oxides. *Aip Advances,* 2(3):032146, 2012.

[19] Uran, S., Alhani, A. and Silva, C. Study of ultraviolet-visible light absorbance of exfoliated graphite forms. *Aip Advances,* 7(3):035323, 2017.

[20] Fu, C., Zhao, G., Zhang, H. and Li, S. Evaluation and characterization of reduced graphene oxide nanosheets as anode materials for lithium-ion batteries. *Int. J. Electrochem. Sci,* 8(5):6269-6280, 2013.

[21] Manoratne, C., Rosa, S. and Kottegoda, I. XRD-HTA, UV visible, FTIR and SEM interpretation of reduced graphene oxide synthesized from high purity vein graphite. *Mater. Sci. Res. India,* 14(1):19-30, 2017.

[22] Long, J., Li, S., Liang, J., Wang, Z. and Liang, B. Preparation and characterization of graphene oxide and it application as a reinforcement in polypropylene composites. *Polymer Composites,* 40(2):723-729, 2019.

[23] Shao, G., Lu, Y., Wu, F., Yang, C., Zeng, F. and Wu, Q. Graphene oxide: the mechanisms of oxidation and exfoliation. *Journal of materials science,* 47(10):4400-4409, 2012.

[24] Lerf, A., He, H., Forster, M. and Klinowski, J. Structure of graphite oxide revisited. *The Journal of Physical Chemistry B,* 102(23):4477-4482, 1998.

[25] Ansari, M. Z., Johari, R. and Siddiqi, W. A. Novel and green synthesis of chemically reduced graphene sheets using Phyllanthus emblica (Indian Gooseberry) and its photovoltaic activity. *Materials Research Express,* 6(5):055027, 2019.

[26] Furst, A., Berlo, R. C. and Hooton, S. Hydrazine as a reducing agent for organic compounds (catalytic hydrazine reductions). *Chemical Reviews,* 65(1):51-68, 1965.

[27] Wang, G., Yang, J., Park, J., Gou, X., Wang, B., Liu, H. and Yao, J. Facile synthesis and characterization of graphene nanosheets. *The Journal of Physical Chemistry C,* 112(22):8192-8195, 2008.

[28] Akhavan, O., Kalaee, M., Alavi, Z., Ghiasi, S. M. A. and Esfandiar, A. Increasing the antioxidant activity of green tea polyphenols in the presence of iron for the reduction of graphene oxide. *Carbon,* 50(8):3015-3025, 2012.

[29] Wang, Y., Shi, Z. and Yin, J. Facile synthesis of soluble graphene via a green reduction of graphene oxide in tea solution and its biocomposites. *ACS applied materials & interfaces,* 3(4):1127-1133, 2011.

[30] Shubha, P., Namratha, K., Aparna, H. S., Ashok, N., Mustak, M. S., Chatterjee, J. and Byrappa, K. Facile green reduction of graphene oxide using Ocimum sanctum hydroalcoholic extract and evaluation of its cellular toxicity. *Materials Chemistry and Physics,* 198:66-72, 2017.

[31] Kuila, T., Bose, S., Khanra, P., Mishra, A. K., Kim, N. H. and Lee, J. H. A green approach for the reduction of graphene oxide by wild carrot root. *Carbon,* 50(3):914-921, 2012.

[32] Thakur, S. and Karak, N. Green reduction of graphene oxide by aqueous phytoextracts. *Carbon,* 50(14):5331-5339, 2012.

[33] Akhavan, O., Ghaderi, E., Abouei, E., Hatamie, S. and Ghasemi, E. Accelerated differentiation of neural stem cells into neurons on ginseng-reduced graphene oxide sheets. *Carbon,* 66:395-406, 2014.

[34] Li, C., Zhuang, Z., Jin, X. and Chen, Z. A facile and green preparation of reduced graphene oxide using Eucalyptus leaf extract. *Applied Surface Science,* 422:469-474, 2017.

[35] Maddinedi, S. B., Mandal, B. K., Vankayala, R., Kalluru, P. and Pamanji, S. R. Bioinspired reduced graphene oxide nanosheets using Terminalia chebula seeds extract. *Spectrochimica Acta Part A: Molecular and Biomolecular Spectroscopy,* 145:117-124, 2015.

[36] Fernández-Merino, M. J., Guardia, L., Paredes, J., Villar-Rodil, S., Solís-Fernández, P., Martínez-Alonso, A. and Tascón, J. Vitamin C is an ideal substitute for hydrazine in the reduction of graphene oxide suspensions. *The Journal of Physical Chemistry C,* 114(14):6426-6432, 2010.

[37] Chong, S. W., Lai, C. W. and Hamid, S. B. A. Green preparation of reduced graphene oxide using a natural reducing agent. *Ceramics International,* 41(8):9505-9513, 2015.

[38] Chu, H.-J., Lee, C.-Y. and Tai, N.-H. Green reduction of graphene oxide by Hibiscus sabdariffa L. to fabricate flexible graphene electrode. *Carbon*, 80:725-733, 2014.

[39] Gao, J., Liu, F., Liu, Y., Ma, N., Wang, Z. and Zhang, X. Environment-friendly method to produce graphene that employs vitamin C and amino acid. *Chemistry of materials,* 22(7):2213-2218, 2010.

[40] Akhavan, O., Ghaderi, E., Aghayee, S., Fereydooni, Y. and Talebi, A. The use of a glucose-reduced graphene oxide suspension for photothermal cancer therapy. *Journal of Materials Chemistry,* 22(27):13773-13781, 2012.

[41] Zhu, C., Guo, S., Fang, Y. and Dong, S. Reducing sugar: new functional molecules for the green synthesis of graphene nanosheets. *ACS nano,* 4(4):2429-2437, 2010.

[42] Esfandiar, A., Akhavan, O. and Irajizad, A. Melatonin as a powerful bio-antioxidant for reduction of graphene oxide. *Journal of Materials Chemistry,* 21(29):10907-10914, 2011.

[43] Liu, J., Fu, S., Yuan, B., Li, Y. and Deng, Z. Toward a universal "adhesive nanosheet" for the assembly of multiple nanoparticles based on a protein-induced reduction/decoration of graphene oxide. *Journal of the american chemical society,* 132(21):7279-7281, 2010.

[44] Akhavan, O. and Ghaderi, E. Escherichia coli bacteria reduce graphene oxide to bactericidal graphene in a self-limiting manner. *Carbon,* 50(5):1853-1860, 2012.

[45] Akhavan, O. Bacteriorhodopsin as a superior substitute for hydrazine in chemical reduction of single-layer graphene oxide sheets. *Carbon,* 81:158-166, 2015.

[46] Akhavan, O., Azimirad, R., Gholizadeh, H. and Ghorbani, F. Hydrogen-rich water for green reduction of graphene oxide suspensions. *International Journal of hydrogen energy,* 40(16):5553-5560, 2015.

[47] Hatamie, S., Akhavan, O., Sadrnezhaad, S. K., Ahadian, M. M., Shirolkar, M. M. and Wang, H. Q. Curcumin-reduced graphene oxide sheets and their effects on human breast cancer cells. *Materials Science and Engineering: C,* 55:482-489, 2015.

[48] Si, Y. and Samulski, E. T. Synthesis of water soluble graphene. *Nano letters,* 8(6):1679-1682, 2008.

[49] Shan, C., Yang, H., Han, D., Zhang, Q., Ivaska, A. and Niu, L. Water-soluble graphene covalently functionalized by biocompatible poly-L-lysine. *Langmuir,* 25(20):12030-12033, 2009.

[50] Ali, M., Rumpa, N.-E. N., Paul, S., Hossen, M., Tanvir, E., Hossan, T., Saha, M., Alam, N., Karim, N. and Khalil, M. Antioxidant potential, subacute toxicity, and beneficiary effects

of methanolic extract of pomelo (Citrus grandis L. Osbeck) in long evan rats. *Journal of Toxicology*, 2019, 2019.

[51] Xu, G., Liu, D., Chen, J., Ye, X., Ma, Y. and Shi, J. Juice components and antioxidant capacity of citrus varieties cultivated in China. *Food chemistry,* 106(2):545-551, 2008.

[52] Toh, J., Khoo, H. and Azrina, A. Comparison of antioxidant properties of pomelo [Citrus Grandis (L) Osbeck] varieties. *International Food Research Journal,* 20(4), 2013.

[53] Israel, K. S., Murthy, C., Patil, B. and Hosamani, R. Value addition of tamarind products in Karnataka. *Journal of Pharmacognosy and Phytochemistry,* 8(6):726-730, 2019.

[54] Soong, Y.-Y. and Barlow, P. J. Antioxidant activity and phenolic content of selected fruit seeds. *Food chemistry,* 88(3):411-417, 2004.

[55] Ugwuona, F. and Onweluzo, J. Assessment of antioxidant properties of tamarind fruit pulp and its effect on storage stability of African bread fruit seed dhal and flour. *Nigerian Food Journal,* 31(2):41-47, 2013.

[56] Panicker, N. J., Das, J. and Sahu, P. Synthesis of highly oxidized graphene (HOG) by using HNO3 and KMnO4 as oxidizing agents. *Materials Today: Proceedings,* 46:6270-6274, 2021.

[57] Stankovich, S., Dikin, D. A., Piner, R. D., Kohlhaas, K. A., Kleinhammes, A., Jia, Y., Wu, Y., Nguyen, S. T. and Ruoff, R. S. Synthesis of graphene-based nanosheets via chemical reduction of exfoliated graphite oxide. *Carbon,* 45(7):1558-1565, 2007.

[58] Tung, V. C., Allen, M. J., Yang, Y. and Kaner, R. B. High-throughput solution processing of large-scale graphene. *Nature nanotechnology,* 4(1):25-29, 2009.

[59] Sadhukhan, S., Ghosh, T. K., Rana, D., Roy, I., Bhattacharyya, A., Sarkar, G., Chakraborty, M. and Chattopadhyay, D. Studies on synthesis of reduced graphene oxide (RGO) via green route and its electrical property. *Materials Research Bulletin,* 79:41-51, 2016.

[60] Sadhukhan, S., Ghosh, T. K., Roy, I., Rana, D., Bhattacharyya, A., Saha, R., Chattopadhyay, S., Khatua, S., Acharya, K. and Chattopadhyay, D. Green synthesis of cadmium oxide decorated reduced graphene oxide nanocomposites and its electrical and antibacterial properties. *Materials Science and Engineering: C,* 99:696-709, 2019.

[61] Shen, J., Li, T., Shi, M., Li, N. and Ye, M. Polyelectrolyte-assisted one-step hydrothermal synthesis of Ag-reduced graphene oxide composite and its antibacterial properties. *Materials Science and Engineering: C,* 32(7):2042-2047, 2012.

[62] Gililland, J. M., Anderson, L. A., Erickson, J., Pelt, C. E. and Peters, C. L. Mean 5-year clinical and radiographic outcomes of cementless total hip arthroplasty in patients under the age of 30. *BioMed research international,* 2013, 2013.

[63] Upadhyay, R. K., Soin, N., Bhattacharya, G., Saha, S., Barman, A. and Roy, S. S. Grape extract assisted green synthesis of reduced graphene oxide for water treatment application. *Materials Letters,* 160:355-358, 2015.

[64] Ganguly, A., Sharma, S., Papakonstantinou, P. and Hamilton, J. Probing the thermal deoxygenation of graphene oxide using high-resolution in situ X-ray-based spectroscopies. *The Journal of Physical Chemistry C,* 115(34):17009-17019, 2011.

[65] Yu, H., Zhang, B., Bulin, C., Li, R. and Xing, R. High-efficient synthesis of graphene oxide based on improved hummers method. *Scientific reports,* 6(1):1-7, 2016.

[66] Kudin, K. N., Ozbas, B., Schniepp, H. C., Prud'Homme, R. K., Aksay, I. A. and Car, R. Raman spectra of graphite oxide and functionalized graphene sheets. *Nano letters,* 8(1):36-41, 2008.

[67] Zhan, D., Ni, Z., Chen, W., Sun, L., Luo, Z., Lai, L., Yu, T., Wee, A. T. S. and Shen, Z. Electronic structure of graphite oxide and thermally reduced graphite oxide. *Carbon,* 49(4):1362-1366, 2011.

[68] Li, B., Jin, X., Lin, J. and Chen, Z. Green reduction of graphene oxide by sugarcane bagasse extract and its application for the removal of cadmium in aqueous solution. *Journal of Cleaner Production,* 189:128-134, 2018.

[69] Li, J., Liu, C.-y. and Liu, Y. Au/graphene hydrogel: synthesis, characterization and its use for catalytic reduction of 4-nitrophenol. *Journal of Materials Chemistry,* 22(17):8426-8430, 2012.

[70] Pesika, N. S., Stebe, K. J. and Searson, P. C. Determination of the particle size distribution of quantum nanocrystals from absorbance spectra. *Advanced Materials,* 15(15):1289-1291, 2003.

[71] Loh, K. P., Bao, Q., Eda, G. and Chhowalla, M. Graphene oxide as a chemically tunable platform for optical applications. *Nature chemistry,* 2(12):1015-1024, 2010.

[72] Cui, P., Lee, J., Hwang, E. and Lee, H. One-pot reduction of graphene oxide at subzero temperatures. *Chemical Communications,* 47(45):12370-12372, 2011.

[73] Yang, H., Shan, C., Li, F., Han, D., Zhang, Q. and Niu, L. Covalent functionalization of polydisperse chemically-converted graphene sheets with amine-terminated ionic liquid. *Chemical Communications,* (26):3880-3882, 2009.

[74] Lee, G. and Kim, B. S. Biological reduction of graphene oxide using plant leaf extracts. *Biotechnology progress,* 30(2):463-469, 2014.

[75] Jiang, L., Yao, M., Liu, B., Li, Q., Liu, R., Lv, H., Lu, S., Gong, C., Zou, B. and Cui, T. Controlled synthesis of CeO2/graphene nanocomposites with highly enhanced optical and catalytic properties. *The Journal of Physical Chemistry C*, 116(21):11741-11745, 2012.